The Astrophysical Journal, 649: L133–L136, 2006 October 1

ENCELADUS: A SOURCE OF NITROGEN AND AN EXPLANATION FOR THE WATER VAPOR PLUME OBSERVED BY *CASSINI*

M. J. Loeffler, U. Raut, and R. A. Baragiola[1]
University of Virginia, Laboratory for Atomic and Surface Physics, Engineering Physics, Charlottesville, VA 22904;
mjl8r@virginia.edu, ur5n@virginia.edu, raul@virginia.edu
Received 2006 May 31; accepted 2006 August 16; published 2006 September 19

ABSTRACT

Recently, the *Cassini* spacecraft observed an unexpected emission of plumes of water vapor, nitrogen, and icy particles from the southern polar region of Saturn's icy moon Enceladus. While these findings support previous ideas of geological activity in this icy moon, there is no experimental evidence explaining how these plumes could be produced at the low (~130–160 K) surface temperatures. Here we show that similar behavior appears when heating water-ammonia ices that have been irradiated with protons that simulate Saturn's energetic ion environment. In our experiments, the behavior results from the eruption of high-pressure bubbles of hydrogen and nitrogen molecules that accumulate in the ice due to the radiolytic decomposition of ammonia. The thermal release of nitrogen can explain the intriguing finding of N^+ in the inner magnetosphere. Thus, our laboratory simulations indicate that radiation processing of the surface of Enceladus may explain much of the extraordinary phenomena that have been observed by *Cassini*.

Subject headings: infrared: general — methods: laboratory — planets and satellites: individual (Enceladus, Saturn) — radiation mechanisms: general

Online material: color figures

1. INTRODUCTION

The measurements of *Voyager*, remote sensing, and more recently the *Cassini* spacecraft have shown unique conditions at and around Enceladus. The surface of this satellite is the brightest and most diverse among the Saturnian satellites (Porco et al. 2006; Verbiscer et al. 2005). Furthermore, the densest part of the E-ring and a neutral OH torus fall near the orbit of Enceladus, suggesting that they originate from sources in this satellite (Jurac et al. 2001a). Besides water and its dissociation products, *Cassini* detected nitrogen from an unknown source near Enceladus (Smith et al. 2005; Young et al. 2005). Recent fly-bys have shown temperatures as high as 145 K near the South Pole (Spencer et al. 2006), much higher than the subsolar temperature (~80 K; Spencer et al. 2006). In addition, *Cassini* detected a spectacular fountain of water ice particles and vapor emanating from this South Polar region (Hansen et al. 2006; Porco et al. 2006; Spahn et al. 2006; Waite et al. 2006). This is astounding since, even at 145 K, water evaporates at a rate (Sack & Baragiola 1993) that is many orders of magnitude slower than that needed to entrain particles observed in this fountain.

The origin of the thermal anomalies, water bursts, nitrogen in the inner magnetosphere, E-ring particles, and OH torus remains largely unexplained. Since the first measurements of *Voyager*, it has been thought that Enceladus is geologically active (Smith et al. 1982; Squyres et al. 1983) due to an uncertain heat source (Porco et al. 2006) that could melt a subsurface material, such as a solid solution of water and ammonia (Lewis 1971), which has an eutectic point of 173 K at the dihydrate composition (NH_3-$2H_2O$). It has been postulated that this heat source could be provided by tidal heating (Ross & Schubert 1989; Squyres et al. 1983) that could be enhanced by an orbital resonance (Wisdom 2004), since radiogenic heating may be insufficient on Enceladus (Ellsworth & Schubert 1983; Squyres et al. 1983) even though it may lead to local melting and structural changes in the ice by decay of radiogenic species in the interior of the moon (Prialnik & Bar-Nun 1990). The liquid melted by this heat source could surface occasionally when cracks open, producing new smooth terrain, or burst out in cryovolcanism (Kargel & Pozio 1996), which could feed the E-ring. Since Enceladus is embedded in Saturn's magnetosphere, ion irradiation may preferentially remove ammonia (or its components) by sputtering (Lanzerotti et al. 1984), which would allow a much lower NH_3 concentration on the surface (Brown et al. 2006; Emery et al. 2005; Verbiscer et al. 2006) than in the bulk. The effects of magnetospheric ion irradiation are evident in the chemical alteration of the surfaces of satellites of Jupiter (Carlson et al. 1999) and other satellites of Saturn (Noll et al. 1997). Here we present laboratory studies of ion irradiation and thermal annealing of water—ammonia mixtures applicable to Enceladus and possibly to other objects in the outer solar system.

2. EXPERIMENTAL SETUP

The experiments were performed in vacuum at 2×10^{-10} torr using a mass-analyzed beam of 100 keV protons. Solid ammonia-water films were grown at 80 K on the gold mirror surface of a quartz-crystal microbalance (QCM) to a thickness of ~2 μm (148 μg cm^{-2}), slightly larger than the depth of penetration of the ions (Ziegler 2003). The mixtures were grown using two separate gas dosers with the 1 : 2 NH_3 : H_2O ratio of the dihydrate, as this is one of the equilibrium phases for ice mixtures with <65.4 percent by weight ammonia (Hogenboom et al. 1997). The samples were then annealed to 120 K to achieve uniform mixing. Irradiations were done at 70 K while monitoring the samples with infrared reflectance (1.5–15 μm), a mass spectrometer (MS) aimed at the surface, and gravimetry using the microbalance. More details on the experimental setup can be found in Loeffler et al. (2006a).

[1] Corresponding author.

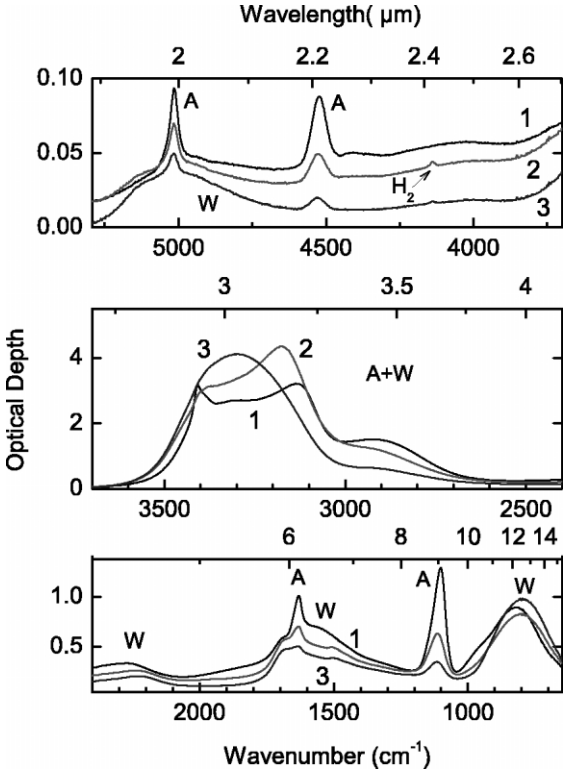

FIG. 1.—The 1 : 2 ammonia-water mixture at 70 K (1) before and (2) after irradiation with 2.45 × 10^{15} H^+ cm^{-2} and (3) 9.5 × 10^{15} H^+ cm^{-2} at 100 keV. Features are labeled as W for water and A for ammonia. [*See the electronic edition of the Journal for a color version of this figure*.]

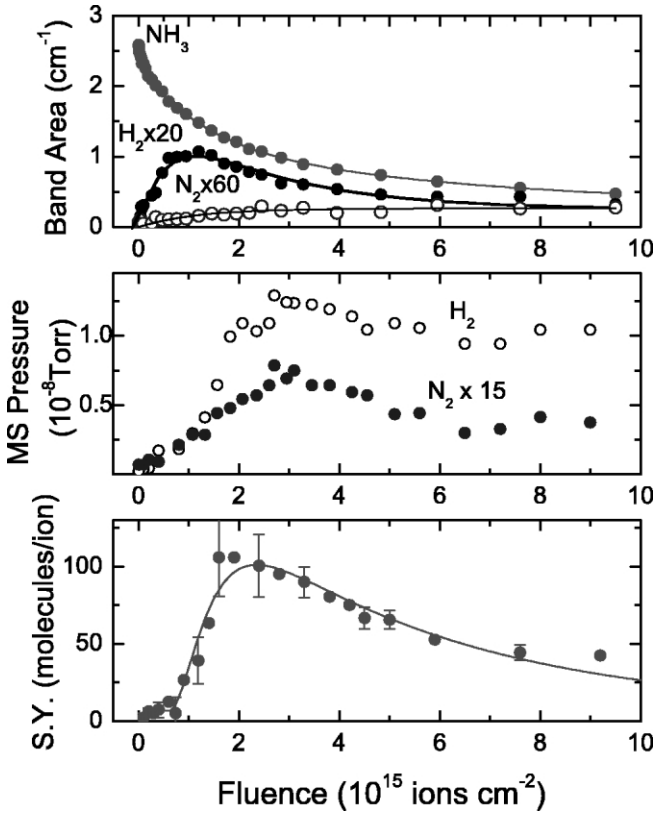

FIG. 2.—Evolution of a 1 : 2 ammonia-water mixture during irradiation with 100 keV protons at 70 K. *Top*: Fluence dependence of the infrared band area of NH_3, H_2, and N_2. *Middle*: Raw data of gas ejection measured by the mass spectrometer. *Bottom*: Sputtering yield averaged over different experiments. The sputtering yield was calculated by dividing the mass loss by 17 amu. The lines shown are to guide the eye. [*See the electronic edition of the Journal for a color version of this figure*.]

3. RESULTS

3.1. *Effects Seen During Irradiation*

Figure 1 shows the evolution of the infrared spectra of an ice mixture during irradiation. The spectra are dominated by water and ammonia features but also contain a weak band at 4139 cm^{-1} from H_2 and a ~20 times weaker band at 2325 cm^{-1} from N_2. These dipole transitions in H_2 and N_2 are forbidden for the free molecules; their appearance is likely due to symmetry breaking perturbations at defect sites (e.g., molecules trapped at vacancies). The fluence dependence of the band areas of infrared transitions for NH_3 (4523 cm^{-1}), H_2, and N_2 are shown in Figure 2 (*top*); the initial drop in NH_3 agrees with the low-fluence measurements of Strazzulla & Palumbo (1998). The mass loss measured by the microbalance during the course of this experiment shows that <30% of the ammonia is removed by ion impact (sputtering). Thus, the 81% drop in the NH_3 band area is not only due to sputtering but mainly due to the decomposition of the molecule and formation of radiation products trapped in the ice, which include H_2 and N_2 (Fig. 2, *top*). The two lower panels in Figure 2 show the fluxes of ejected H_2 and N_2 measured by the MS, and the total sputtering yield, defined as the number of molecules ejected per incident ion. These quantities increase with fluence peaking at ~(2–3) × 10^{15} ions cm^{-2}, suggesting that they are related to the accumulation of trapped species, such as H, H_2, N, NH_x, and N_2. Although the MS signal due to the NH_3 is masked by OH from the water background, we were able to monitor the NH cracking product with the MS and found it to be below the noise level during irradiation, indicating that ejection of intact NH_3 molecules or NH_x fragments is a minor contributor to sputtering. The drop in the sputtering yield and the MS signals at high fluences is correlated with the depletion of the radiolytic products (and ammonia) inside the film. We note that these processes do not have a thermal origin, since interruption of irradiation stopped changes in the infrared spectra, the outgassing flux, and the mass loss.

3.2. *Effects Seen During Post-Irradiation Warming*

To explore the effects of temperature changes on the irradiated ices, we warmed the samples at 0.2 K $minute^{-1}$ after irradiation, while measuring the infrared spectra, the mass loss, and the flux of the desorbed gas (Fig. 3). The H_2 and N_2 band areas decrease steadily during warming, even though there are no corresponding changes in the QCM and MS between 70 and 115 K. Since this decrease in the band area is not due to a loss of molecules, it is likely related to the annealing of defects that enabled these dipole forbidden transitions, as has been seen for O_2 in condensed gases (Loeffler et al. 2006b).

During warming we observed two types of gas ejection: the usual thermal outgassing and strikingly fast (≤100 ms) bursts occurring at a frequency that peaks at ~125 K and ceases by ~130 K. The mass loss from the sample during each burst was below our level of detection (~3 ng), but there was a cumulative loss of 14.2 μg cm^{-2} due to these bursts and the underlying broad desorption peak. The bursts observed in the total flux, as is seen in the flickering of the ionization gauge, and in MS signals are due to hydrogen, nitrogen, and water. The broad desorption peak contains mainly water and H_2 with little nitrogen; we note that this desorption peak corresponds to an 8% drop in the area of

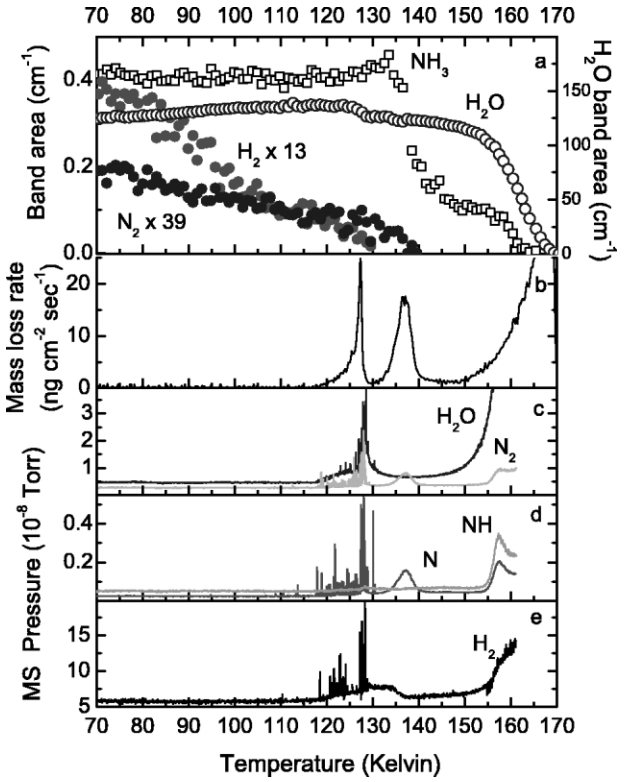

FIG. 3.—Evolution of a 1 : 2 ammonia-water sample irradiated with 7.5×10^{15} H^+ cm^{-2} at 70 K during warming at 0.2 K minute^{-1}. (*a*) Band areas calculated from the infrared spectra, (*b*) mass-loss rate from microbalance (ng cm^{-2} s^{-1}), and (*c*–*e*) pressure reading in the MS uncorrected for relative efficiencies. The MS data are not plotted beyond 161 K because it includes molecules coming from surfaces outside the irradiated area. [*See the electronic edition of the Journal for a color version of this figure.*]

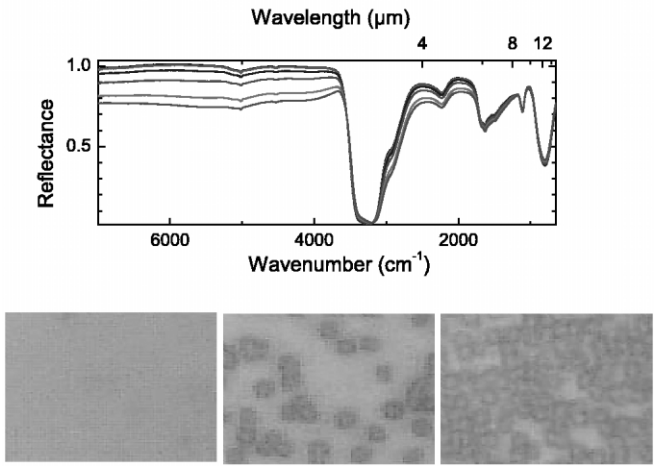

FIG. 4.—*Top*: Evolution of the infrared reflectance of a 1 : 2 ammonia-water sample deposited on a gold substrate and irradiated by 7.5×10^{15} H^+ cm^{-2} at 70 K during warming at 0.2 K minute^{-1}. The decrease in reflectance above 4000 cm^{-1} is seen at increasing temperatures (*from top to bottom*) of 108, 118, 122, 125, 127, and 129 K. *Bottom*: Micrographs of the sample after irradiation before warming (*left*), in the beginning of the bursts (*middle*), and near the end of the bursts (*right*). The scale of the micrographs is 50 × 36 μm. [*See the electronic edition of the Journal for a color version of this figure.*]

the water absorption band at ~800 cm^{-1} (Fig. 3, *top*) The next peak in the mass-loss rate, at 137 K, is correlated with the emission of nitrogen, and contains 22.1 μg cm^{-2} or 51% of the mass of nitrogen (in NH_3) in the film before irradiation. This loss of nitrogen at this temperature is nearly 5 times larger than that due to the decrease of ammonia, inferred from the drop of the infrared absorption band at the top of Figure 3. As seen for other gases (see, e.g., Vidal et al. 1997) this broad N_2 peak occurs during crystallization of the water ice that remains in the sample, possibly as a result of the enhanced diffusion paths along the newly formed grain boundaries. At higher temperatures, the small drop of the NH_3 absorption band and the increase of the NH signal in the MS due to NH_3 cracking indicate desorption of the ammonia that remained trapped in the ice after crystallization. We note that there is no emission of intact ammonia molecules below 140 K.

The peak in the desorption of water, seen between 115 and 130 K, was unexpected, because in both pure water ice (Sack & Baragiola 1993) and in an unirradiated mixture, this degree of sublimation is only seen at much high temperatures. This desorption peak is not directly related to H_2 accumulation in the ice, since the fluence (1.2×10^{15} ions cm^{-2}) that maximizes trapped H_2 (Fig. 2) is significantly smaller than that for maximum water desorption (7.5×10^{15} ions cm^{-2}). Since the water desorption peak is always accompanied by outbursts of H_2 and N_2, we propose that these gases aggregate as gas bubbles of increasingly higher pressure inside radiation-induced voids in the ice (Loeffler et al. 2006b). We note that trapped gas is expected to accumulate to nearly solid-state densities, implying pressures as high as 1000 atmospheres. Similarly to what occurs in the trapping of gases in nuclear fusion reactors (Das & Kaminsky 1976; Gittus 1978), when the gas pressure exceeds the fracture strength of the ice, gas in surface blisters bursts out exfoliating the blister top, resulting in the ejection of vapor and small ice particles. Although of a different origin, this mechanism is similar to the ejection of icy particles from gas-loaded ice during warming (Laufer et al. 1987). When the blisters rupture, they scatter light causing a decrease in the reflectance of the sample, as shown in Figure 4 (*top*). The resulting surface topography has been photographed in situ with a long distance microscope, Figure 4 (*bottom*), showing the appearance of features on the order of 5 μm across. The ejected particles could be smaller since the blister top could break into smaller pieces when the ice ruptures, of the order of the micron size E-ring particles deduced by Showalter et al. (1991) through the modeling of *Voyager* photometric data.

4. ASTROPHYSICAL IMPLICATIONS

At Enceladus, a layer of ammonia dihydrate that resurfaces by some endogenic process will be irradiated by magnetospheric protons to an energy fluence of 1×10^{18} keV cm^{-2} (corresponding to 1×10^{16} 100 keV ions cm^{-2}) in ~25 yr, using data from Jurac et al. (2001b). This time is probably a lower limit since the flux may be an overestimate (Paranicas et al. 2004). Magnetospheric ion irradiation will deplete the surface of ammonia, making improbable its detection by infrared reflectance (Brown et al. 2006; Emery et al. 2005; Verbiscer et al. 2006) until the next resurfacing event occurs. Irradiation also causes ejection of hydrogen and nitrogen from the surface. In particular, the nitrogen emission explains the observation of N^+ near Enceladus by the *Cassini* Plasma Spectrometer (CAPS; Smith et al. 2005; Young et al. 2005) and of the neutral N_2 observed by the *Cassini* Ion and Neutral Mass Spectrometer (INMS; Waite et al. 2006).

The desorption of water vapor and ejection of icy particles at temperatures as low as 115 K can explain the plume of gas

and particles emitted from the South Polar region of Enceladus observed by the *Cassini* Ultraviolet Imaging Spectrograph (UVIS; Hansen et al. 2006). Scaling our results for desorbed gas between 100 and 130 K to the size of the region responsible for the plume, estimated from the images (Porco et al. 2006) to be 2.4×10^4 km^2, leads to $\sim 3.4 \times 10^8$ kg of ejected material where we have taken into account that higher energy ions and electrons will alter the surface material to depths ~100 times larger than 100 keV ions (Cooper et al. 2001). This number gives our plume a lifetime of ~25 days using the escape rate of 150 kg s^{-1} estimated by Hansen et al. (2006). This number of days, although possibly sufficient to explain a sporadic plume compatible with the variability of the Saturnian environment (Esposito et al. 2005; Porco et al. 2006), is certainly a lower limit for the lifetime of the plume. Gardening of the regolith, as has been observed in the Moon, will occur by impacts of micrometeorites, including ice grains from the rings, burying and mixing the radiolytic products to depths much larger than the penetration range of the energetic particles. The effect of this turnover will be to substantially increase the thickness of the ammonia depletion region and the lifetime of the plumes. In addition, if the decay of radioactive elements turns out to be a significant source of heat, it will also enhance the decomposition of ammonia and the formation of radiolytic products, possibly throughout the ice mantle.

This research was supported by NASA Planetary Atmospheres and *Cassini* program and by NSF Astronomy. M. J. L. thanks the Virginia Space Grant Consortium for a fellowship.

REFERENCES

Brown, R. H., et al. 2006, Science, 311, 1425
Carlson, R. W., et al. 1999, Science, 283, 2062
Cooper, J. F., Johnson, R. E., Mauk, B. H., Garrett, H. B., & Gehrels, N. 2001, Icarus, 149, 133
Das, S. K., & Kaminsky, M. 1976, Adv. Chem. Ser., 158, 112
Ellsworth, K., & Schubert, G. 1983, Icarus, 54, 490
Emery, J. P., Burr, D. M., Cruikshank, D. P., Brown, R. H., & Dalton, J. B. 2005, A&A, 435, 353
Esposito, L. W., et al. 2005, Science, 307, 1251
Gittus, J. 1978, Irradiation Effects in Crystalline Solids (London: Appl. Sci.)
Hansen, C. J., et al. 2006, Science, 311, 1422
Hogenboom, D. L., Kargel, J. S., Consolmagno, G. J., Holden, T. C., Lee, L., & Buyyounouski, M. 1997, Icarus, 128, 171
Jurac, S., Johnson, R. E., & Richardson, J. D. 2001a, Icarus, 149, 384
Jurac, S., Johnson, R. E., Richardson, J. D., & Paranicas, C. 2001b, Planet. Space Sci., 49, 319
Kargel, J. S., & Pozio, S. 1996, Icarus, 119, 385
Lanzerotti, L. J., Brown, W. L., Marcantonio, K. J., & Johnson, R. E. 1984, Nature, 312, 139
Laufer, D., Kochavi, E., & Bar-Nun, A. 1987, Phys. Rev. B, 36, 9219
Lewis, J. S. 1971, Icarus, 15, 174
Loeffler, M. J., Teolis, B. D., & Baragiola, R. A. 2006a, J. Chem. Phys., 124, 104702
Loeffler, M. J., Teolis, B. D., & Baragiola, R. A. 2006b, ApJ, 639, L103
Noll, K. S., Roush, T. L., Cruikshank, D. P., Johnson, R. E., & Pendleton, Y. J. 1997, Nature, 388, 45
Paranicas, C., Decker, R. B., Mauk, B. H., Krimigis, S. M., Armstrong, T. P., & Jurac, S. 2004, Geophys. Res. Lett., 31, L04810
Porco, C. C., et al. 2006, Science, 311, 1393
Prialnik, D., & Bar-Nun, A. 1990, ApJ, 355, 281
Ross, M. N., & Schubert, G. 1989, Icarus, 78, 90
Sack, N. J., & Baragiola, R. A. 1993, Phys. Rev. B, 48, 9973
Showalter, M. R., Cuzzi, J. N., & Larson, S. M. 1991, Icarus, 94, 451
Smith, B. A., et al. 1982, Science, 215, 505
Smith, H. T., et al. 2005, Geophys. Res. Lett., 32, L14S03
Spahn, F., et al. 2006, Science, 311, 1416
Spencer, J. R., et al. 2006, Science, 311, 1401
Squyres, S. W., Reynolds, R. T., Cassen, P. M., & Peale, S. J. 1983, Icarus, 53, 319
Strazzulla, G., & Palumbo, M. E. 1998, Planet. Space Sci., 46, 1339
Verbiscer, A. J., French, R. G., & McGhee, C. A. 2005, Icarus, 173, 66
Verbiscer, A. J., et al. 2006, Icarus, 182, 211
Vidal, R. A., Bahr, D., Baragiola, R. A., & Peters, M. 1997, Science, 276, 1839
Waite, J. H., et al. 2006, Science, 311, 1419
Wisdom, J. 2004, AJ, 128, 484
Young, D. T., et al. 2005, Science, 307, 1262
Ziegler, J. F. 2003, Stopping and Range of Ions in Matter: SRIM-2003, http://www.srim.org